Substitution mechanisms in In, Au, and Cu-bearing sphalerites studied by X-ray absorption spectroscopy of synthetic and natural minerals

Filimonova, O. N.; Trigub, A. L.; Tonkacheev, D. E.; Nickolsky, M. S.; Kvashnina, K. O.; Chareev, D. A.; Chaplygin, I. V.; Kovalchuk, E. V.; Lafuerza, S.; Tagirov, B. R.;

Originally published:

March 2019

Mineralogical Magazine 83(2019)3, 435-451

DOI: https://doi.org/10.1180/mgm.2019.10

Physics and Chemistry of Minerals

The coupled chemistry of In and Au in sphalerites studied by X-ray absorption spectroscopy of synthetic crystals

--Manuscript Draft--

Manuscript Number:	
Full Title:	The coupled chemistry of In and Au in sphalerites studied by X-ray absorption spectroscopy of synthetic crystals
Article Type:	Original paper
Keywords:	Indium; gold; trace elements; sphalerite; synthetic minerals; HERFD-XAS; EXAFS
Corresponding Author:	Boris Tagirov Institute of geology of ore deposits, petrography, mineralogy and geochemistry (IGEM RAS) RUSSIAN FEDERATION
Corresponding Author Secondary Information:	
Corresponding Author's Institution:	Institute of geology of ore deposits, petrography, mineralogy and geochemistry (IGEM RAS)
Corresponding Author's Secondary Institution:	
First Author:	Olga Filimonova
First Author Secondary Information:	
Order of Authors:	Olga Filimonova
	Dmitry Tonkacheev
	Boris Tagirov
	Alexander Trigub
	Maksimilian Nickolsky
	Kristina Kvashnina
	Sara Lafuerza
	Dmitry Chareev
Order of Authors Secondary Information:	
Funding Information:	Russian Science Foundation (14-17-00693) — Not applicable
	Russian Foundation for Basic Research (16-05-00938) — Dr Dmitry Chareev
Abstract:	Processing of Zn ore accounts for >95% of production of In - a "critical" metal which is widely used in the high-tech electronics. The main source of In is sphalerite (Zn, Fe)S which also can host industrial concentrations of Au. Here we use X-ray absorption spectroscopy to investigate the coupled chemistry of In and Au in synthetic sphalerite crystals - analogues of natural minerals. The concentrations of In and Au were found to correlate with each other and reached 0.5 wt% in crystals synthesized at 850 °C. Both metals are homogeneously distributed within the sphalerite matrix. However, their positions within the mineral are different. In accord with X-ray absorption near edge structure (XANES) spectroscopy the formal oxidation state of these elements is +3 (In) and +1 (Au). Analysis of extended X-ray absorption fine structure (EXAFS) spectra revealed that In replaces Zn in the structure of sphalerite. The In-ligand distance increases by 0.12 Å and 0.09-0.10 Å for the 1st and 2nd coordination spheres, respectively, in comparison with pure ZnS. The In-S distance in the 3rd coordination sphere is close to the one of pure sphalerite. The In K-edge and Au L3-edge XANES and EXAFS spectra suggest that there is no In-Au clustering. Gold in sphalerite is

	coordinated with 2.5±0.3 S atoms at Au-S distance of 2.35±0.01 Å in the 1st coordination sphere, whereas distant coordination spheres have disordered nature. Our data suggest that at least two different forms of Au are present in sphalerite. At high Au concentrations (0.03-0.5 wt%) the nanosized Au2S clusters predominate, probably with small admixture of the Au solid solution characterized by higher Au-S distance. Alike Au, the other 1st group metals (Me) Cu and Ag, which often are present in high (tenths ppm to wt%) concentrations in sphalerite, can form nanosized Me-S clusters with only traces (ppm level) of metal in the solid solution state.

The coupled chemistry of In and Au in sphalerites studied by X-ray absorption spectroscopy of synthetic crystals

O.N. Filimonova[1], D.E. Tonkacheev[1], B.R. Tagirov[1*], A.L. Trigub[1,2], M.S. Nickolsky[1], K.O. Kvashnina[3,7], S. Lafuerza[3], D.A. Chareev[4,5,6]

[1] Institute of Geology of Ore Deposits (IGEM RAS), 35, Staromonetnyi per., 119017 Moscow, Russia

[2] National Research Centre 'Kurchatov Institute', 1 Akademika Kurchatova pl., 123182 Moscow, Russisa

[3] ESRF - The European Synchrotron, CS40220, 38043 Grenoble Cedex 9, France

[4] Institute of Experimental Mineralogy (IEM RAS), 142432 Chernogolovka, Moscow Region, Russia

[5] Institute of Physics and Technology, Ural Federal University, Mira st., 19, 620002 Ekaterinburg, Russia

[6] Institute of Geology and Petroleum Technologies, Kazan Federal University, Kremlyovskaya, 4/5, 420008, Kazan, Russia.

[7] Helmholtz-Zentrum Dresden-Rossendorf (HZDR), Institute of Resource Ecology, P.O. Box 510119, 01314, Dresden, Germany.

***Corresponding author:** e-mail boris1t@yandex.ru; phone +7-499-2308231

Submitted to Physics and Chemistry of Minerals September 2017

Acknowledgments The authors acknowledge the ESRF for the beamtime allocation under proposals 20-01-782 (ROBL) and ES-184 (ID26), and STM beamline team (KSRS) for technical support during the experiment. The help and support of Joerg Exner (ROBL) during the beam time is greatly appreciated. We are grateful to V. Abramova and E. Minervina for chemical analyses of synthesized minerals using LA-ICP-MS methods, E. Kovalchuk for EPMA analyses. Chemical analyses were performed at the "IGEM-Analytica" laboratory. This study was supported by the Russian Science Foundation grant No. 14-17-00693 (XAS experiments and data treatment) and Russian Foundation for Basic Research grant No. 16-05-00938 (crystal growth experiments). The work of DACh was supported by the program 211 of the Russian Federation Government, agreement No. 02.A03.21.0006, and by the Russian Government Program of Competitive Growth of Kazan Federal University.

Abstract

Processing of Zn ore accounts for >95% of production of In – a "critical" metal which is widely used in the high-tech electronics. The main source of In is sphalerite (Zn, Fe)S which also can host industrial concentrations of Au. Here we use X-ray absorption spectroscopy to investigate the coupled chemistry of In and Au in synthetic sphalerite crystals - analogues of natural minerals. The concentrations of In and Au were found to correlate with each other and reached 0.5 wt% in crystals synthesized at 850 °C. Both metals are homogeneously distributed within the sphalerite matrix. However, their positions within the mineral are different. In accord with X-ray absorption near edge structure (XANES) spectroscopy the formal oxidation state of these elements is +3 (In) and +1 (Au). Analysis of extended X-ray absorption fine structure (EXAFS) spectra revealed that In replaces Zn in the structure of sphalerite. The In-ligand distance increases by 0.12 Å and 0.09-0.10 Å for the 1^{st} and 2^{nd} coordination spheres, respectively, in comparison with pure ZnS. The In-S distance in the 3^{rd} coordination sphere is close to the one of pure sphalerite. The In K-edge and Au L_3-edge XANES and EXAFS spectra suggest that there is no In-Au clustering. Gold in sphalerite is coordinated with 2.5±0.3 S atoms at Au-S distance of 2.35±0.01 Å in the 1^{st} coordination sphere, whereas distant coordination spheres have disordered nature. Our data suggest that at least two different forms of Au are present in sphalerite. At high Au concentrations (0.03-0.5 wt%) the nanosized Au_2S clusters predominate, probably with small admixture of the Au solid solution characterized by higher Au-S distance. Alike Au, the other 1^{st} group metals (Me) Cu and Ag, which often are present in high (tenths ppm to wt%) concentrations in sphalerite, can form nanosized Me-S clusters with only traces (ppm level) of metal in the solid solution state.

Keywords: Indium; gold; trace elements; sphalerite; synthetic minerals; HERFD-XAS; EXAFS

Introduction

Indium is a critical metal which is of high demand in high-tech industries. It is used worldwide for the production of flat-panel displays and touchscreens, in the manufacturing of photovoltaic cells, fiber-optics, and has some other important industrial applications (Mercer 2015). The global primary production of In increased almost twofold during 2001-2011, and totaled 759 t in 2015 and 655 t in 2016 (Tolchin 2017). The concentration of In in natural environments is low and, therefore, In minerals are rare. Instead, it is concentrated in the principal sulfide ore-forming minerals among which sphalerite (Zn, Fe)S is the most important (Schwartz-Schampera 2015). The In content in sphalerite usually falls within 0.1-100 ppm range, but can reach several wt% in minerals formed at high temperatures (400 - 725 °C) in volcanic fumaroles (Chaplygin et al. 2007). Often the concentration of In is directly correlated with concentration of Cu which implies the formation of solid solution by the coupled substitution mechanism $2Zn^{2+} \leftrightarrow Cu^{+} + In^{3+}$ (Chaplygin et al. 2007; Cook et al. 2009).

Indium is recovered as a byproduct of mining and refinement of Zn ore. The most significant sources of In are sulfide Zn- and Zn-Cu ores of volcanogenic base metal-sulfide (VMS) deposits (Mercer 2015; Schwartz-Schampera 2015). Many of these deposits and their modern analogues – ores of submarine hydrothermal fields, are Au-rich (Bortnikov et al. 2003; Melekestseva et al. 2017). Some VMS deposits belong to world-class gold mines with more than 100 t Au (e.g., Mercier-Langevin et al. 2011; Vikentyev et al. 2004, 2015). Determination of Au concentration in submarine polymetallic sulfide ore from the Valu Fa Ridge (the Lau basin, south-west Pacific) showed that the Au-bearing assemblages are dominated by Fe-poor sphalerite (Herzig et al. 1993). Gold is present in sphalerites of VMS deposits of the Urals in concentrations from *n* to *n*·10 ppm (Vikentyev 2015). Particles of Au were often observed on the grains of In-bearing sphalerite and wurtzite crystals deposited in the fumarolic system of Kudriavy volcano (Iturup Island, Russia, Chaplygin et al. 2007). Thus, both In and Au are closely associated in natural environments and can be extracted as byproduct commodities from sphalerite-bearing sulfide ores.

Investigation of spectroscopic properties of pure and doped ZnS, as well as the chemical speciation of the impurities (dopants), is mostly driven by useful technical applications of these materials (see, for example, Inorganic phosphors: composition, preparation, and optical properties 2004). Recently, doped semiconductor nanocrystals (quantum dots) have drawn significant attention due to their unique electronic and optical properties (Norris et al. 2008). Apple and Williams (1959) and Koelmans (1960) synthesized and studied ZnS phosphors activated with In and first-group metals (Ag, Cu). It was suggested that the formation of In-

bearing hexagonal ZnS (wurtzite) takes place by the charge compensation mechanism which corresponds to the replacement of 3 Zn^{2+} ions by 2 In^{3+} ions and the formation of one Zn vacancy (Koelmans 1960). Incorporation of In resulted in substantial increase of the ZnS lattice constants which confirmed the solid solution formation. However, slow cooling from the synthesis temperature or reheating to t > 600 °C killed fluorescence of the material. The lattice spacings of these samples were found to be equal to those of pure ZnS. Association of charged In^{3+} ion and negatively charged Zn^{2+} vacancy was suggested to be responsible for the emission drop and the lattice constants decrease. Therefore, the suggested charge compensation scheme seems to be pertinent only when In-bearing ZnS is rapidly quenched from the formation (synthesis) temperature, whereas slow cooling or reheating (metamorphism) of natural ores can result in redistribution of charges. Note that the coupled In-Cu substitution is not the necessary condition for the formation of In-bearing sphalerites because both Cu- and In-bearing ZnS materials were synthesized separately for technical applications.

The atomic and electronic structures of synthetic sphalerites doped with Mn, Fe, Co, and Ni were studied using X-ray absorption spectroscopy (XAS) in Ławniczak-Jabłońska et al. (1994, 1995, 1996) and Iwanowski et al. (1996, 1997, 1998). The authors showed that these impurities are incorporated into the cationic position of the sphalerite lattice, evaluated the Me-S distances in the doped sulfide, and calculated tetrahedral covalent radii of the dopants. Pattrick et al. (1998) studied local atomic structure of sphalerites doped with Mn, Cu/In, and Cd. The concentration of $CuInS_2$ in synthesized sphalerites was 8-20 at%. It was found that these metals are incorporated into the sphalerite cationic sublattice, and the S tetrahedra around the dopant are compressed for Cu and expanded for In and other dopants. Besides, the authors determined that In/In and Cu/In clustering occurs at these high concentrations of dopants (note that much lower admixture concentrations are pertinent for natural sphalerites).

The solid solution model for Cu was not, however, confirmed in more recent XAS studies of doped materials with lower Cu content. The local atomic structure of ZnS phosphors doped with Cu and Mn was studied by extended X-ray absorption fine structure (EXAFS) spectroscopy in Warkentin et al. (2007). An important issue of this study is that Mn substitutes for Zn in cubic ZnS lattice, whereas Cu is present in the ZnS matrice mainly in the form of nanosized CuS clusters with only small fraction of Cu substituting for Zn. Based on the EXAFS data analysis, the CuS nanocrystallites are suggested to be integrated into the ZnS matrix and "do not have a completely random orientation, i.e. there is not an amorphous layer between the CuS-like nanocrystallites and the host crystal" (Warkentin et al. 2007). The formation of CuS nanosized precipitates in the ZnS matrix was confirmed by EXAFS study of Cu-doped ZnS nanoclusters reported in Corrado et al. (2009). The XAS studies of trace elements (Ge, Cu, Mn)

in natural sphalerites are limited to the X-ray near edge structure (XANES) spectra because of small gain size, their zonal character, and low concentration of the admixtures (Cook et al. 2015, Bonnet et al. 2016, 2017).

Recently we found that the concentration of Au in sphalerite increases with increasing In content (Tonkacheev et al. 2015). In the present study, in order to determine the speciation of In and Au in sphalerite, we introduced these impurities into synthetic pure and Fe-bearing sphalerites and studied the synthesized crystals by means of XAS. The use of synthetic crystals with elevated concentrations of admixtures made possible to acquire not only XANES spectra, but to obtain good quality EXAFS and, as a result, unambiguously determine the local atomic environment of In and Au. An important advantage of the use of Au – the heaviest 1st group stable atom, is that in the case of In-Au clustering the contribution of this atom to the In K-edge EXAFS can be recognized by the spectra analysis in contrast to light atom of Cu, which can not be discriminated from Zn or Fe. For Au the High energy resolution fluorescence detection mode was employed (HERFD-XAS, Glatzel and Bergman 2005). The measurement of HERFD-XANES spectra allowed observation of important spectral features not manifested in total fluorescence yield (TFY) detection (Tagirov et al. 2016; Trigub et al. 2017). Our experimental results demonstrate that in sphalerite In exists in the solid solution state, whereas Au, despite homogeneous distribution and possibility of charge compensation substitution, mostly forms nanosized Au_2S clusters with only small fraction of the Au solid solution.

Experimental

Methods of synthesis

The crystal growth experiments were performed as described in Chareev et al. (2017) using i) gas transport method, and ii) salt flux technique (KCl/NaCl eutectic mixture, Chareev 2016, Chareev et al. 2016). In gas transport method NH_4Cl was used as a transport agent. The initial phases (~ 0.5 g of ZnS – wurtzite, with 3-5 wt% FeS), and, if necessary, several milligrams of MnS, CdS, ZnSe, and In_2S_3 were powdered and loaded into a silica glass ampoule (8 mm ID, 11 mm OD, ~110 mm length) together with Au wire and either ~ 5 mg of transport agent or salt flux which filled the rest of the ampoule volume. The loaded ampoules were evacuated, sealed, and placed into a horizontal tube furnace which was then heated to the synthesis temperature over a period of 2-3 hours, and then kept at this temperature during 20-30 days. The temperature gradient in the furnace was 50-100 °C, and the measured temperature at the hot end of the ampoules was 850 °C. At the end of the experiment the ampoules were quenched in cold water. Sphalerite crystals precipitated at the cold end.

Gold sulfide $Au_2S_{(cr)}$ was synthesized by sulfidizing aqueous Au cyanide solution at

ambient temperature as described in Tagirov et al. (2006).

Analytical methods

Morphology of the synthesized minerals was checked using scanning electron microscopy (SEM), phase composition was obtained by means of X-ray diffraction (XRD), chemical composition was determined with electron probe micro-analysis (EPMA) and laser ablation inductively coupled mass spectrometry (LA-ICP-MS). The JSM-5610LV microscope equipped with INCA-450 energy dispersive spectrometer was used for SEM studies. EPMA analyses were performed using JEOL JXA-8200 WD/ED combined electron probe microanalyzer equipped with 5 wavelength dispersive X-ray spectrometers. For major elements (Cu, Fe, S) the operating conditions were 20 kV accelerating voltage, 20 nA beam current, with a counting time of 10 s. Zinc, Fe, and S were determined using K_α lines with LiF (for Zn, Fe) and PETH (for S) crystals. Chalcopyrite $CuFeS_2$ (for Fe) and pure sphalerite ZnS (for Zn and S) were used as the calibration reference materials. Indium was determined using L_α line and PETH crystal with 20 kV accelerating voltage and 20 nA beam current, counting time of 10 s. The InSb was used as a reference material. The concentration of Au was determined using LiF crystal accounting for the background dip immediately adjacent to the Au L_α line from the short-wavelength side (Self et al., 1990). Limit of detection (2σ) for Au was 0.01 wt% at 100 nA beam current and counting time of 100 s.

Concentrations of ^{197}Au and ^{113}In isotopes in the synthesized sphalerite crystals, and the distribution modes (homogeneous/inhomogeneous) of Au and In were checked using LA-ICP-MS. The New Wave 213 laser coupled with the Thermo X Series2 quadrupole ICP-MS was used. The laser frequency was 10 Hz with the power of 6-8 J/cm^2 and beam size of 40-60 μm. The analysis was carried out during 30 s preceded by 20 s for the gas blank. The ablation was performed in He + 6% H_2 (0.6 L/min) atmosphere. The gas carrying ablated material to the ICP-mass spectrometer was mixed with Ar (0.8 L/min). Sulfide reference material MASS-1 (Wilson et al. 2002) was used as an external calibration standard for both In and Au together with in-house pyrrhotite $Fe_{0.9}S$ (18 ppm Au, synthesized using method from Wohlgemuth-Ueberwasser et al. (2007) and calibrated at the Université Québec à Chicoutimi (UQAC) with respect to concentration of Au against standard prepared by J.H.G. Laflamme). Isotopes ^{68}Zn or ^{33}S were used as internal standards. Detection limit for Au (2σ) was 0.1 ppm. Scan speed of 5 μm/s was used for analyses along lines.

X-ray absorption spectroscopy

X-ray absorption experiments were performed at the European Synchrotron Radiation Facility (ESRF) in Grenoble, France; and Kurchatov Synchrotron Radiation Source (KSRS) in Moscow, Russia.

The Au L_3-edge spectra were collected at the high-brilliance X-ray absorption/X-ray emission spectroscopy undulator beamline ID26 (Gauthier et al. 1998) of the ESRF. The storage-ring operating conditions were 6.0 GeV and the ring current was varied between 150 and 200 mA. The incident energy was selected using the <111> reflection from a double Si crystal monochromator. Rejection of higher harmonics was achieved by three Pd mirrors positioned at an angle of 2.5 mrad relative to the incident beam. The incident X-ray beam had a flux of approximately $2 \cdot 10^{13}$ photons s^{-1} on sample position. The spectra were measured in high energy resolution fluorescence detection (HERFD) mode using an X-ray emission spectrometer (Glatzel and Bergman 2005; Kvashnina and Scheinost 2016). The sample, analyzer crystal and photon detector (silicon drift diode) were arranged in a vertical Rowland geometry. The Au L_3-edge HERFD-XAS spectra were obtained by recording the intensity of the Au $L_{\alpha 1}$ emission line (9713 eV) as a function of the incident energy. The emission energy was selected using the <555> reflection of four spherically bent Ge crystal analyzers (1 m curvature radius) aligned at 78° Bragg angle. A combined (incident convoluted with emitted) energy resolution of 1.5 eV was determined as the full width at half maximum of the elastic peak. The intensity was normalized to the incident flux.

The In K-edge spectra were recorded at the Rossendorf Beamline BM20 of the ESRF. The storage-ring operating conditions were 6.0 GeV and 80-100 mA. The photon energy was scanned from 27700 to 28570 eV using the Si(111) monochromator coupled to Rh-coated mirrors for the collimation and reduction of higher harmonics. Energy calibration was performed using the K-edge excitation energy of In metal foil (27940 eV). The spectra for reference substances were collected in transmission mode while for sphalerite samples the spectra were recorded in total fluorescence yield (TFY) mode using 13-element high-throughput Ge-detector. The total energy resolution (incident energy and core − hole lifetime broadening) has been evaluated as 8.8 eV. The detected intensity was normalized to the incident photon flux.

The Zn and Fe K-edge spectra were measured at the Structural Materials Science station (Chernyshov et al. 2009) of the KSRS. The storage-ring operating conditions were 2.3 GeV and 80-100 mA. A Si(111) monochromator was used and the energy calibration was performed using the K-edge absorption energy of Zn and Fe foils. The X-ray absorption spectra of Zn were registered in transmission mode and the spectra of Fe in fluorescence mode using an avalanche photodiode (FMB OXFORD).

EXAFS spectra fitting

The EXAFS ($\chi_{exp}(k)$) data were analyzed using IFEFFIT package (Ravel and Newville 2005). Following standard procedures for pre-edge subtraction and spline background removal, the structural parameters - interatomic distances (R_i), coordination numbers (N_i), and Debye–Waller factors (σ^2_i) - were determined via the non-linear fit of theoretical spectra to the experimental ones with the equation

$$\chi(k) = S_0^2 \sum_{i=1}^{n} \frac{N_i F_i(k)}{R_i^2 k} e^{\frac{-2R_i}{\lambda(k)}} e^{-2\sigma_i^2 k^2} \sin(2kR_i + \varphi_i(k)) \quad . \quad (1)$$

Theoretical spectra were simulated using photoelectron mean free path $\lambda(k)$, amplitude $F_i(k)$, and phase shift $\varphi_i(k)$ parameters calculated *ab initio* using the program FEFF6 (Zabinsky et al. 1995).

In addition, the Au L_3-edge spectra were fit with the aid of Reverse Monte Carlo (RMC) method. The advantage of this method in comparison with the ARTEMIS program (a part of IFEFFIT software package) is that it allows one to perform accurate analysis of EXAFS data from distant coordination spheres, taking into account both multiple-scattering and disorder (thermal and static) effects (e.g., Rossberg and Scheinost 2005; Timoshenko et al. 2012, 2017). In this case the atomic structure of a material is generated through random displacements of atoms in order to minimize the difference between experimental and theoretically calculated EXAFS spectra. EXAFS spectrum of every random atomic configuration was calculated using ab initio real-space multiple-scattering code FEFF8.5L (Ankudinov et al. 1998). To fit the experimental spectra the least square minimization of difference between calculated and experimental $\chi(k)\cdot k^2$ values was performed. These data allow calculation of the radial density $\rho(R)$ of surrounding atoms which is related to coordination numbers N via expression

$$N(R) = \int_0^R 4\pi r^2 \rho(R) dr \quad . \quad (2)$$

Results and discussion

Concentration and distribution of In and Au

As a result of the synthesis experiments aggregates of crystals with grain size $n\cdot 0.1 - 1$ mm were obtained (an example of the synthesis product is shown in Fig. 1). The XRD pattern of synthesized samples corresponded to pure sphalerite phase PDF#5-566. Chemical composition of crystals is listed in Table 1. High-temperature sphalerites synthesized at 850 °C incorporated extremely high (up to 0.5 wt%) concentrations of both In and Au. Both In and Au were found to be dispersed in the state “invisible” by optical and electron microscopies. The concentrations of these admixtures in the synthesized crystals are close to each other and directly correlated.

Homogeneous In and Au distribution patterns are confirmed by small scatter of measured concentrations (see uncertainties of measured concentrations given in Table 1) and smooth character of LA-ICP-MS time-resolved spectra (Fig. 2).

XANES spectroscopy

The In K-edge XANES and Au L_3-edge HERFD-XANES spectra of sphalerite samples are compared to the reference substances in Fig. 3, and energy positions of the edge jump (e.j.) and the first intense feature known as white line (WL) are listed in Table 2.

In K-edge

For all In-bearing sphalerites the e.j. and WL positions of In K-edge spectra are identical independently of the concentration of In, Fe, and Au. This means that the concentration of Fe, Au, and In itself, has negligible effect on the chemical state (local atomic environment and the valence state) of In. At the same time, the e.j. and WL positions are different from those of the In_2O_3 and In_2S_3: they are shifted by 0.7-1 eV to lower energies in comparison with In_2O_3, and, on the contrary, by ~1 eV to higher energies compared to In_2S_3 (Table 2). Accordingly, the chemical state of indium in sphalerite is different from oxide and sulfide.

We may interpret the observed e.j. energy position in the spharelites by saying that the oxidation state of In is intermediate between In_2O_3 and In_2S_3; however, the formal oxidation state of In in sphalerite is +3. The higher energy of the e.j. position in In-bearing sphalerite in comparison with In_2S_3 can be ascribed to stronger In-S interaction in the state of the solid solution, which results in a more effective negative charge transfer from In to S. The latter would result in a shorter In-S distance in In-bearing sphalerite compared to In_2S_3. Additional reason in favor of the compression of the 1st coordination sphere is that the minima of the XANES spectra, which separates WL and the 2nd spectral feature, is located at much higher energy of ~27980 eV for In-bearing sphalerite than for In_2S_3 (~27972 eV).

Au L_3-edge

The Au L_3-edge HERFD-XANES spectra of sphalerites differ from the spectra of Au and Au_2S. The e.j. and WL positions are shifted to higher energies compared to the Au_2S spectra. Position of the second spectral feature also exhibits large positive shift by ~3 eV. The low WL intensity in comparison with Au^{3+} state (e.g., Tagirov et al. 2016) suggests that the formal oxidation state of Au is +1. The shape of the WL feature of sphalerite spectra, unlike Au_2S, is highly asymmetric which can be explained by the presence of several different geometries of the local atomic environment of Au. At the same time, the shape and positions of the spectral

features are identical for In-rich and In-free sphalerites, which suggests the absence of In/Au clustering. This important conclusion will be checked via EXAFS spectra analysis.

EXAFS spectra fitting

Results of EXAFS spectra fitting obtained using IFEFFIT software package (ARTEMIS program) for Zn, Fe, In K-edges, and for Au L_3-edge are collected in Table 3 and compared with the experimental spectra in Fig. 4a (In K-edge) and 4b (Au L_3-edge). The results of Au L_3-edge RMC fits are shown in Fig. 5.

Fe, Zn K-edges

The local atomic structures around Zn and Fe (coordination numbers and interatomic distances) are identical within the uncertainty of the experimental data, and correspond to pure sphalerite (Zn, Fe)S (top of Table 3). Admixtures of In and Au have no effect on the interatomic distances between Zn/Fe and surrounding atoms.

In K-edge

For In-bearing sphalerites, the best fit of the experimental spectra is achieved when Au substitutes Zn in the sphalerite lattice. In the structure of sphalerite a cation is tetrahedrally coordinated by S atoms; the 2nd coordination sphere consists of 12 Zn atoms, and the 3rd coordination sphere contains 12 S atoms. Preliminary fits of the experimental spectra were performed with calculation of the coordination numbers of atoms in the 2nd and 3rd coordination spheres. The calculated values of *N* fell within the range of 10-19, but the uncertainty of the values was quite large. Therefore, during the final fits these values were fixed in accord with the sphalerite structure parameters ($N = 12$).

Data of Table 3 indicate that the In-S distance increased by 0.12 Å with respect to the crystal structure of pure sphalerite in the 1st coordination sphere, by 0.09-0.1 Å for Zn atoms in the 2nd sphere, whereas the In-S distance for the 3^{d} coordination sphere is close to that of pure ZnS or even slightly decreased (by 0.01 – 0.03 Å which is, however, within the uncertainty of the calculated values). Thus, our data demonstrate that the distortion of the sphalerite crystal structure, caused by the replacement of Zn with In, decreases for distant coordination spheres and disappears at $R > 4.6$ Å. The admixture of Fe in sphalerite (up to 10 wt%) does not change the structural parameters of In. This conclusion is in line with the fact that In K-edge XANES spectra are similar for pure and Fe-bearing sphalerites.

Despite high Au concentrations, we did not observe a contribution of this heavy atom to In K-edge EXAFS spectra up to the 3rd coordination sphere. Therefore, the In-Au clustering is

not necessary for the formation of In solid solution in sphalerite. Generalizing these results to all the 1st group metals one can say that the charge compensation coupled substitution scheme $2Zn^{2+}$ = (Cu, Ag, Au)$^{1+}$ + In^{3+} (e.g., Chaplygin et al. 2007; Cook et al. 2009) takes place without formation of the roquesite $CuInS_2$ or laforetite $AgInS_2$ components in solid solution. This means that In and the 1st group metals are statistically (randomly) distributed within the sphalerite matrix.

Au L_3-edge

In sphalerite the nearest neighbors around Au are S atoms with N_S ~ 2.5. The Au-S distance of 2.35 Å is higher than in Au_2S where Au is linearly coordinated with S atoms (N = 2, $R_{Au\text{-}S}$ = 2.30 Å, Table 3 and Fig. 4b). In contrast to In, for which the structural parameters can be obtained up to 3rd coordination sphere composed by 12 S atoms, the absence of a distinct maxima of the FT for Au L_3-edge EXAFS spectra at R > 2.5 Å (Fig. 4b) implies that the second coordination sphere of Au is of disordered nature. The mentioned values of N and R, complex lineshape of HERFD-XANES spectra with broad asymmetric WL (Fig. 3), as well as disordered distant coordination spheres, can be interpreted as the presence of at least two different forms of Au. This suggestion is confirmed by RMC EXAFS fitting where two peaks of radial density of S at ~2.3 Å (main feature) and ~2.6 Å (weak feature) are present (Fig. 5a,b). Comparing these data with results obtained for Cu-bearing sphalerites (Warkentin et al. 2007) and taking into account similarity of Cu and Au chemical properties, we suggest that these forms can be Au_2S nanosized clusters ($R_{Au\text{-}S}$ ~ 2.3-2.4 Å) and a small admixture of the Au solid solution ($R_{Au\text{-}S}$ ~ 2.6 Å). The pronounced increase by ~ 0.25 Å of the Au-S distance for Au solid solution with respect to the Zn-S distance in sphalerite can be explained by large difference in the ionic radii of these metals (0.6 Å for Zn vs 1.37 Å for Au, Shannon 1976). Our data, however, do not allow to determine if the Au_2S nanosized clusters were formed at the synthesis temperature, or they are a quench product formed by the solid solution decomposition. Alike CuS in Cu-bearing sphalerite (Warkentin et al. 2007), the Au_2S clusters can be integrated into the sphalerite host matrix in accord with the crystallographic axes of the sphalerite structure and, by this way, the metastable gold sulfide can be stabilized. An absence of a contribution from heavy In atom in the distant coordination spheres of Au is an additional argument for the absence of the In-Au clustering. We can speculate that at high temperature Au existed mostly in the solid solution state which decomposed upon cooling with the formation of Au_2S nanosized clusters because i) the concentration of Au in sphalerite is proportional to the In content (these elements can form isomorphous solid solution via the charge compensation scheme), and, ii) Au_2S is a metastable phase which decomposes at high temperature (Tagirov et al. 2006). However, the speciation of

Au in sphalerite at high temperature can be unambiguously determined only by means of in situ spectroscopic experiment performed for sphalerite heated to the formation (synthesis) temperature.

Conclusions

In the present work we synthesized crystals of In and Au-bearing sphalerite (Zn, Fe)S with dopants concentration of 0.03–0.5 wt%. Results of EPMA and LA-ICP-MS chemical analyses showed that both In and Au are homogeneously distributed within the sphalerite matrix. X-ray absorption spectroscopy was applied in order to determine the chemical state (local atomic environment and valence state) of In and Au in synthesized crystals. In accord with XANES spectroscopy these elements are present in sphalerite in +3 (In) and +1 (Au) formal oxidation states. At ambient temperature In is present in sphalerite in the solid solution state where it substitutes for Zn. Analysis of EXAFS spectra shows that the bond length of In increases (relatively to pure ZnS) from 2.34 to 2.46 Å in the 1st coordination sphere where In is tetrahedrally coordinated with S, from 3.83 to 3.92 Å in the 2nd coordination sphere (N_{Zn} = 12), and is close to the Me-S distance of the pure sphalerite for the 3^{d} coordination sphere (N_S = 12, R_{In-S} = 4.46-4.48 Å). Gold, in contrast to In, is mainly present in the form identified as Au_2S nanosized clusters with R_{Au-S} = 2.35 Å, with minor contribution of the second form with R_{Au-S} ~ 2.6 Å which is attributed to the Au solid solution. The second coordination sphere of Au is of disordered nature. These data, together with information published in the literature for Cu-bearing sphalerites, demonstrate that the admixture of the 1st group elements in sphalerite is not necessarily incorporated in the solid solution state, but rather forms Me-S nanosized clusters when the concentration of these elements exceeds ppm level. Hence, the homogeneous character of a trace element distribution, which is often observed in natural sulfide minerals, is not necessarily accounted for by the solid solution formation. Additional experiments with in situ registration of XAS spectra are necessary in order to determine whether the Me^{1+}-S nanosized clusters were formed at the synthesis temperature, or they represent the decomposition product of the In-Me^{1+}-S solid solution which was formed via the charge compensation mechanism by substitution for Zn in the sphalerite structure.

References

Apple EF, Williams FE (1959) Associated donor-acceptor luminescent centers in zinc sulfide phosphors. J Electrochem Soc 106:224-230.

Belissont R, Munoz M, Boiron M-C, Luais B, Mathon O (2016) Distribution and oxidation state of Ge, Cu and Fe in sphalerite by μ-XRF and *K*-edge μ-XANES: insights into Ge incorporation, partitioning and isotopic fractionation. Geochim Cosmochim Acta 177:298-314.

Bonnet J, Cauzid J, Testemale D, Kieffer I, Proux O, Lecomte A, Bailly L (2017) Characterization of germanium speciation in sphalerite (ZnS) from Central and Eastern Tennessee, USA, by X-ray absorption spectroscopy. Minerals 7:79.

Bortnikov NS, Cabri LJ, Vikentiev IV, Tagirov BR, Mc Mahon G, Bogdanov YuA, Stavrova OO (2003) Invisible gold in sulfides from seafloor massive sulfide edifices. Geology of Ore Deposits 45(3):201-212.

Chaplygin IV, Mozgova NN, Mokhov AV, Koporulina EV, Bernardt H-J, Bryzgalov IA (2007) Minerals of the system ZnS-CdS from fumaroles of the Kudriavy volcano, Iturup island, Kuriles, Russia. Can Mineral 45:709-722.

Chareev DA (2016) General principles of the synthesis of chalcogenides and pnictides in salt melts using a steady-state temperature gradient. Crystallography Reports 61(3):506-511.

Chareev DA, Volkova OS, Geringer NV, Koshelev AV, Nekrasov AN, Osadchii VO, Osadchii EG, Filimonova ON (2016) Synthesis of chalcogenide and pnictide crystals in salt melts using a steady-state temperature gradient. Crystallography Reports 61(4):682-691.

Chareev DA, Osadchii VO, Shiryaev AA, Nekrasov AN, Koshelev AV, Osadchii EG (2017) Single-crystal Fe-bearing sphalerite: synthesis, lattice parameter, thermal expansion coefficient and microhardness. Phys Chem Minerals 44:287-296.

Chernyshov AA, Veligzhanin AA, Zubavichus YV (2009) Structural materials science end-station at the Kurchatov Synchrotron Radiation Source: Recent instrumentation upgrades and experimental results. Nucl Instr Meth Phys Res A 603:95-98.

Cook NJ, Etschmann B, Ciobanu CL, Geraki K, Howard DL, Williams T, Rae N, Pring A, Chen G, Johannessen B, Brugger J (2015) Distribution and substitution mechanism of Ge in a Ge-(Fe)-bearing sphalerite. Minerals 5:117-132.

Cook NJ, Ciobanu CL, Pring A, Skinner W, Shimizu M, Danyushevsky L, Melcher F (2009) Trace and minor elements in sphalerite: A LA-ICPMS study. Geochim. Cosmochim. Acta 73:4761-4791.

Corrado C, Jiang Yu, Oba F., Kozina M, Bridges F, Zhang JZ (2009) Synthesis, structural, and optical properties of stable ZnS:Cu,Cl nanocrystals. J Phys Chem A 113:3830-3839.

Glatzel P, Bergman U (2005) High resolution 1s core hole X-ray spectroscopy in 3d transition metal complexes - electronic and structural information. Coord Chem Rev 249:65-95.

Herzig PM, Hannington MD, Fouquet Y, von Stackelberg U, Petersen S (1993) Gold-rich polymetallic sulfides from the Lau back arc and implications for the geochemistry of gold in sea-floor hydrothermal systems of the Southwest Pacific. Econ Geol 88:2182-2209.

Inorganic phosphors: compositions, preparation and optical properties (2004) Yen M, Weber J. (eds). CRC Press.

Ishikawa K, Isonga T, Wakita S, Suzuki Y (1995) Structure and electrical properties of Au_2S. Solid State Ionics 79:60-66.

Iwanowski RJ, Ławniczak-Jabłońska K (1996) EXAFS studies of local atomic structure in $Zn_{1-x}Mn_xS$. Solid State Com 97:879-885.

Iwanowski RJ, Ławniczak-Jabłońska K (1997) EXAFS determination of bond lengths in $Zn_{1-x}Fe_xS$ ternary alloys. Acta Physica Polonica A 91(4):797-801.

Iwanowski RJ, Ławniczak-Jabłońska K, Gołacki Z, Traverse A (1998) Tetrahedral covalent radii of Mn, Fe, Co and Ni estimated from extended X-ray absorption fine structure studies. Chem Phys Let 283:313-318.

Jamieson JC, Demarest HH Jr (1980) A note on the compression of cubic ZnS. J Phys Chem Solids 41:963-964.

Koelmans H (1960) Association and dissociation of centres in luminescent ZnS-In. J Phys Chem Solids 17:69-79.

Ławniczak-Jabłońska K, Gołacki Z (1994) Extended X-ray absorption fine structure studies of Co doped ZnS and ZnSe alloys. Acta Physica Polonica A 86(5):727-735.

Ławniczak-Jabłońska K, Iwanowski RJ, Gołacki Z, Traverse A, Pizzini S, Fontaine A (1995) Correlation between XANES of the transition metals in ZnS and ZnSe and their limit of solubility. Physica B 208&209:497-499.

Ławniczak-Jabłońska K, Iwanowski RJ, Gołacki Z, Traverse A, Pizzini S, Fontaine A, Winter I (1996) Local electronic structure of ZnS and ZnSe doped by Mn, Fe, Co, and Ni from X-ray-absorption near-edge structure studies. Phys Rev B 53:1119-1128.

Melekestseva IYu, Maslennikov VV, Tret'yakov GA, Nimis P, Beltenev VE, Rozhdestvenskaya II, Maslennikova SP, Belogub EV, Danyushevsky L, Large R, Yuminov AM, Sadykov SA (2017) Gold- and silver-rich massive sulfides from the Semenov-2 hydrothermal field, 13°31.13'N, Mid-Atlantic Ridge: a case of magmatic contribution? Econ Geol 112:741–773.

Mercer CN (2015) Indium: bringing liquid-crystal displays into focus. USGS Report Fact Sheet 2015-3012. Reston, VA.

Mercier-Langevin P, Hannington MD, Dubé B, Bécu V (2011) The gold content of volcanogenic massive sulfide deposits. Mineral Deposita 46:509-539.

Norris DJ, Efros AL, Erwin SC (2008). Doped nanocrystals. Nature 319:1776-1779.

Pattrick RAD, Mosselmans JFW, Charnock JM (1998) An X-ray absorption study of doped sphalerites. Eur J Miner 10:239-249.

Ravel B, Newville M (2005) ATHENA, ARTEMIS, HEPHAESTUS: data analysis for X-ray absorption spectroscopy using IFEFFIT. J Synchrotron Rad 12:537-541.

Rehr JJ, Kas JJ, Vila FD, Prange MP, Jorissen K (2010) Parameter-free calculations of X-ray spectra with FEFF9. Phys Chem Chem Phys 12:5503-5513.

Rossberg A, Scheinost AC (2005) Three-dimensional modeling of EXAFS spectral mixtures by combining Monte Carlo simulations and target transformation factor analysis. Anal Bioanal Chem 383:56.

Schwarz-Schampera U (2014) Indium. In: Gunn G (ed) Critical metals handbook. Wiley, pp. 204-229.

Self PG, Norrish K, Milnes AR (1990) Holes in the background in XRS. X-Ray Spectrometry 19:59-61.

Shannon RD (1976) Revised effective ionic radii and systematic studies of interatomic distances in halides and chalcogenides. Acta Cryst A32:751-767.

Tagirov BR, Baranova NN, Zotov AV, Schott J, Bannykh LN (2006) Experimental determination of the stabilities of $Au_2S_{(cr)}$ at 25°C and $Au(HS)_2^-$ at 25-250°C. Geochim Cosmochim Acta 70:3689–3701.

Tagirov BR, Trigub AL, Kvashnina KO, Shiryaev AA., Chareev DA, Nickolsky MS, Abramova VD, Kovalchuk EV (2016) Covellite CuS as a matrix for “invisible” gold: X-ray spectroscopic study of the chemical state of Cu and Au in synthetic minerals. Geochim Cosmochim Acta 191:58–69.

Timoshenko Y, Kuzmin A, Purans Y (2012) Reverse Monte Carlo modeling of thermal disorder in crystalline materials from EXAFS spectra. Comp Phys Comm 183:1237-1245.

Timoshenko Y, Anspoks A, Kalinko A, Kuzmin A. (2017) Thermal disorder and correlation effects in anti-perovskite-type copper nitride. Acta Materialia 129:61-71.

Tolcin AC (2017) Indium. US Geological Survey, Mineral Commodity Summaries, pp. 80-81.

Tonkacheev DE, Chareev DA, Abramova VD, Yudovskaya MA, Minervina EA, Tagirov BR (2015) Sphalerite as a matrix for noble, non-ferrous metals and semimetals: A EPMA and LA-ICP-MS study of synthetic crystals. Proceedings of the 13th Biennial SGA Meeting, 24-27 August 2015, Nancy, France 2:847-850.

Trigub AL, Tagirov BR, Kvashnina KO, Chareev DA, Nickolsky MS, Shiryaev AA, Baranova NN, Kovalchuk EV, Mokhov AV (2017) X-ray spectroscopy study of the chemical

state of “invisible” Au in synthetic minerals in the Fe-As-S system. Am Mineral 102:1057-1065.

Vikentyev IV (2015) Invisible and microscopic gold in pyrite: methods and new data for sulfide ores of the Urals. Geology of Ore Deposits 57(4):237–265.

Vikentyev IV, Yudovskaya MA, Mokhov AV, Kerzin AL, Tsepin AI (2004) Gold and PGE in massive sulphide ore of the Uzelginsk deposit, Southern Urals, Russia. Can Mineral 42:651-665.

Warkentin M, Bridges F, Carter SA, Anderson M (2007) Electroluminescence materials ZnS:Cu,Cl and ZnS:Cu,Mn,Cl studied by EXAFS spectroscopy. Phys Rev B 75:075301.

Wilson SA, Ridley WI, Koenig AE (2002) Development of sulfide calibration standards for the laser ablation inductively-coupled plasma mass spectrometry. J Analyt Atom Spectr 17:406-409.

Wohlgemuth-Ueberwasser CC, Ballhaus C, Berndt J, Stotter née Paliulionyte V, Meisel T. (2007) Synthesis of PGE sulfide standards for laser ablation inductively coupled plasma mass spectrometry (LA-ICP-MS). Contrib Mineral Petrol 154:607-617.

Zabinsky SI, Rehr JJ, Ankudinov A, Albers RC, Eller MJ (1995) Multiple-scattering calculations of X-ray-absorption spectra. Phys Rev B 52:2995.

Figure captions

Figure 1. Optical microscope image of aggregate of sphalerite crystals (Sample 1661). Concentrations of admixtures: 1.9 wt% Fe, 0.22 wt% In, 0.25 wt% Au. FOV 0.3x0.4 mm. Photo by T. Pashko.

Fig. 2. Laser ablation-ICP-MS time-resolved spectra for line analysis across sphalerite grains. Compositions of samples are given in Table 1.

Fig. 3. *Left*: In K-edge XANES spectra of In-Au-bearing sphalerites and model substances (In_2O_3 and In_2S_3). *Right*: Au L_3-edge HERFD-XANES spectra for Au±In-bearing sphalerites and model substances (Au and Au_2S). Vertical dashed lines indicate positions of the most intense spectral features of sphalerite samples.

Fig. 4. In K-edge (a) and Au L_3-edge (b) EXAFS spectra of In-Au-bearing sphalerites, the Au L_3-edge spectra of $Au_2S_{(cr)}$ is shown for comparison. *Top*: k^2-weighted background-subtracted EXAFS spectra, *Bottom*: Fourier transforms (FT) of the k^2-weighted EXAFS spectra (not corrected for phase shift). Black lines – experiment, red lines – fit results. Scattering atoms are indicated near FT peaks, MS – multiple-scattering contributions. Fit results are listed in Table 3.

Fig. 5. Results of RMC fitting, Au L_3-edge EXAFS spectra for In-Au-bearing sphalerites: sample 1450 (a) and sample 1661 (b). *Left*: k^2-weighted background-subtracted EXAFS spectra (points – experimental spectra, red lines – results of RMC fitting); *middle*: Fourier transform of the k^2-weighted EXAFS spectra (not corrected for phase shift); *right*: radial density distribution (blue lines) and coordination numbers (red lines) of Au. Coordination number during the fits was fixed as 2 in assumption that Au_2S predominates. Asymmetric shape of the radial density curve with the second weak maxima at $R \sim 2.6$ Å indicates presence of two different forms of Au.

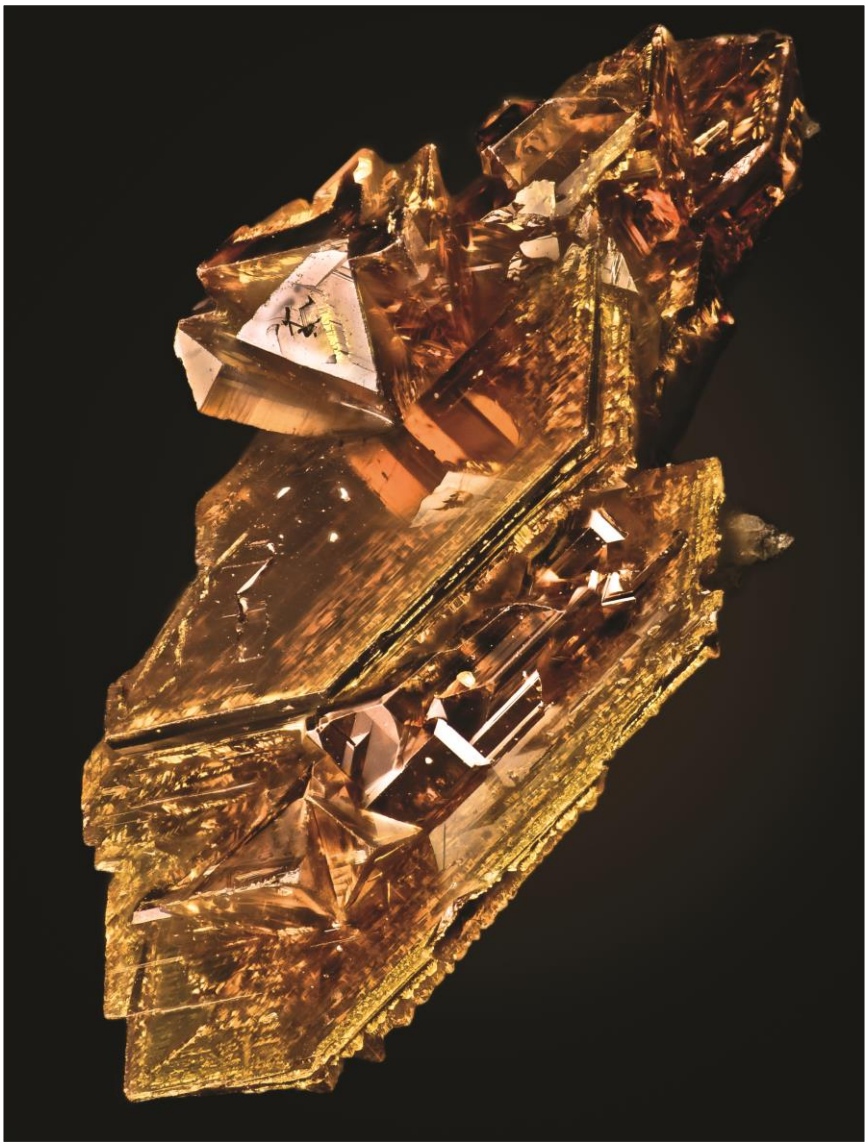

Fig. 1.

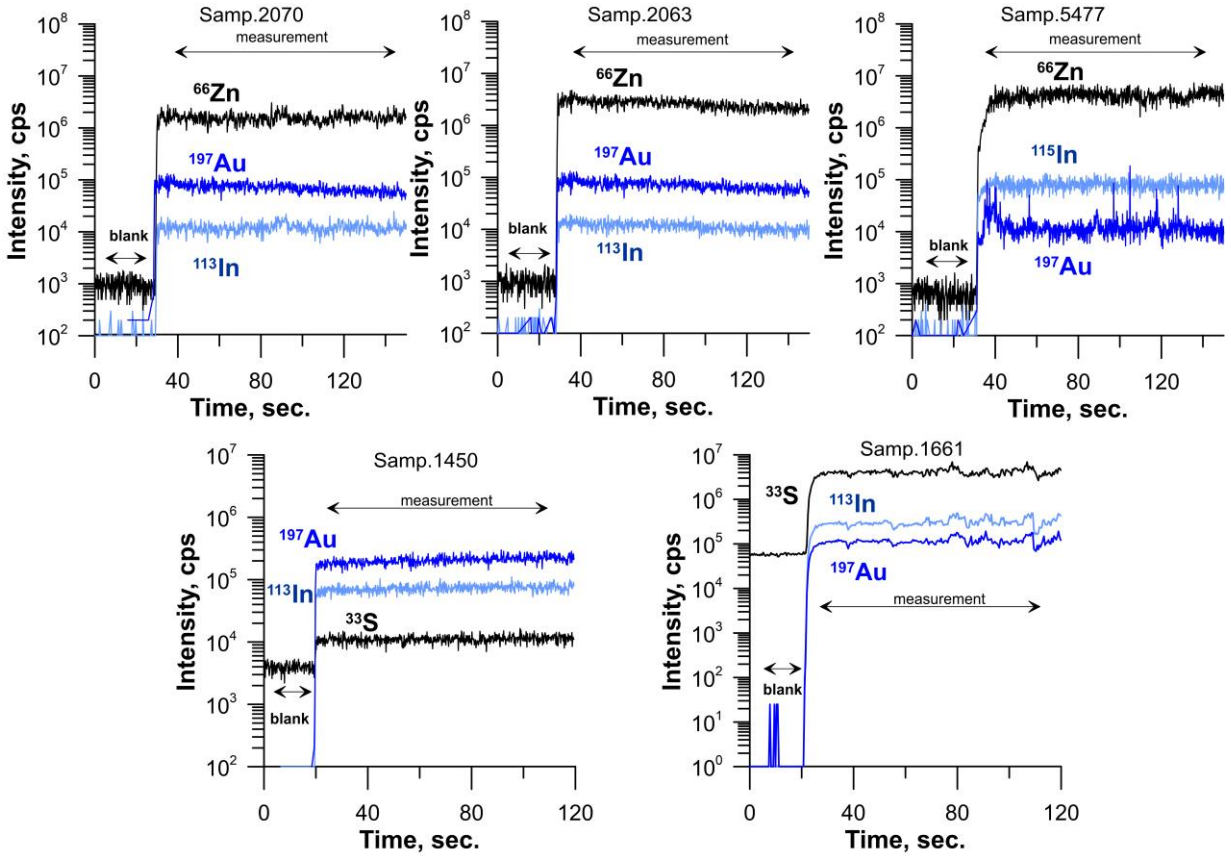
Samp.2070
measurement
66Zn
197Au
113In
blank
Intensity, cps
Time, sec.
Samp.2063
measurement
66Zn
197Au
113In
blank
Intensity, cps
Time, sec.
Samp.5477
measurement
66Zn
115In
197Au
blank
Intensity, cps
Time, sec.
Samp.1450
measurement
197Au
113In
33S
blank
Intensity, cps
Time, sec.
Samp.1661
33S
113In
197Au
measurement
blank
Intensity, cps
Time, sec.

Fig. 2.

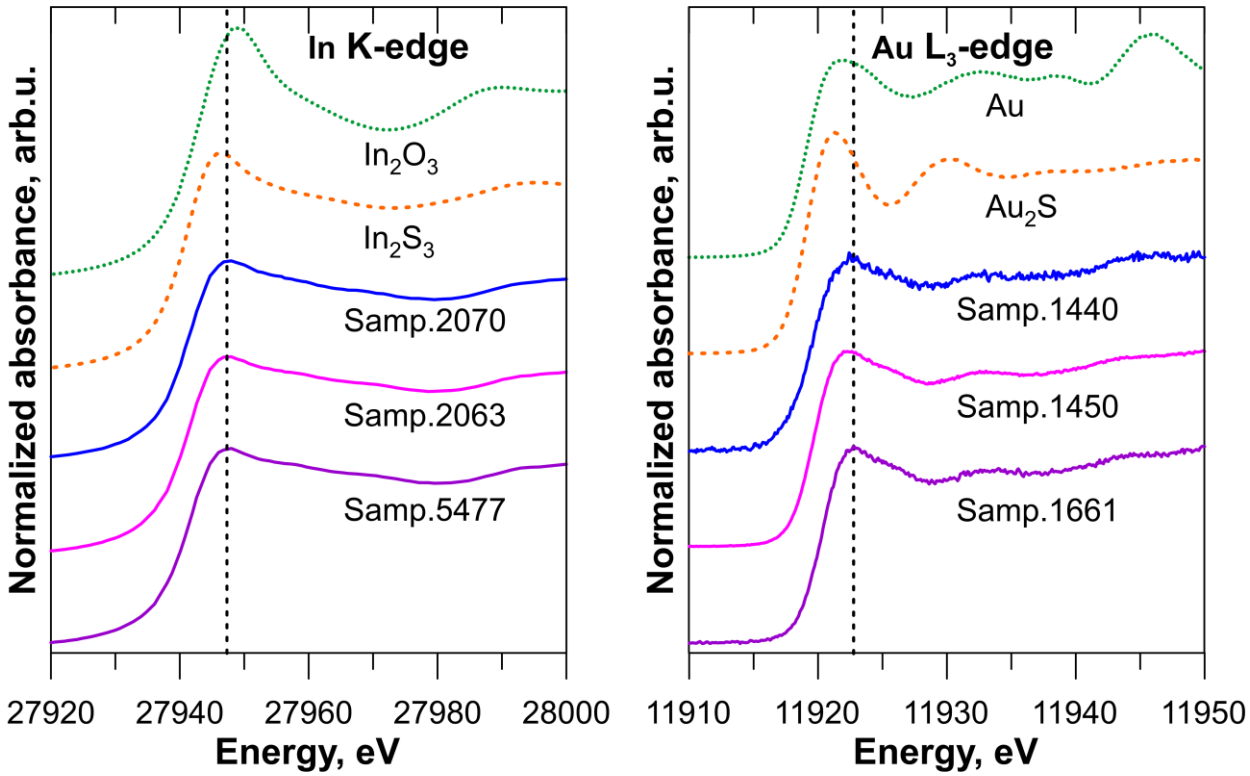
In K-edge
Normalized absorbance, arb.u.
In2O3
In2S3
Samp.2070
Samp.2063
Samp.5477
27920
27940
27960
27980
28000
Energy, eV
Au L3-edge
Au
Au2S
Samp.1440
Samp.1450
Samp.1661
11910
11920
11930
11940
11950
Energy, eV

Fig. 3.

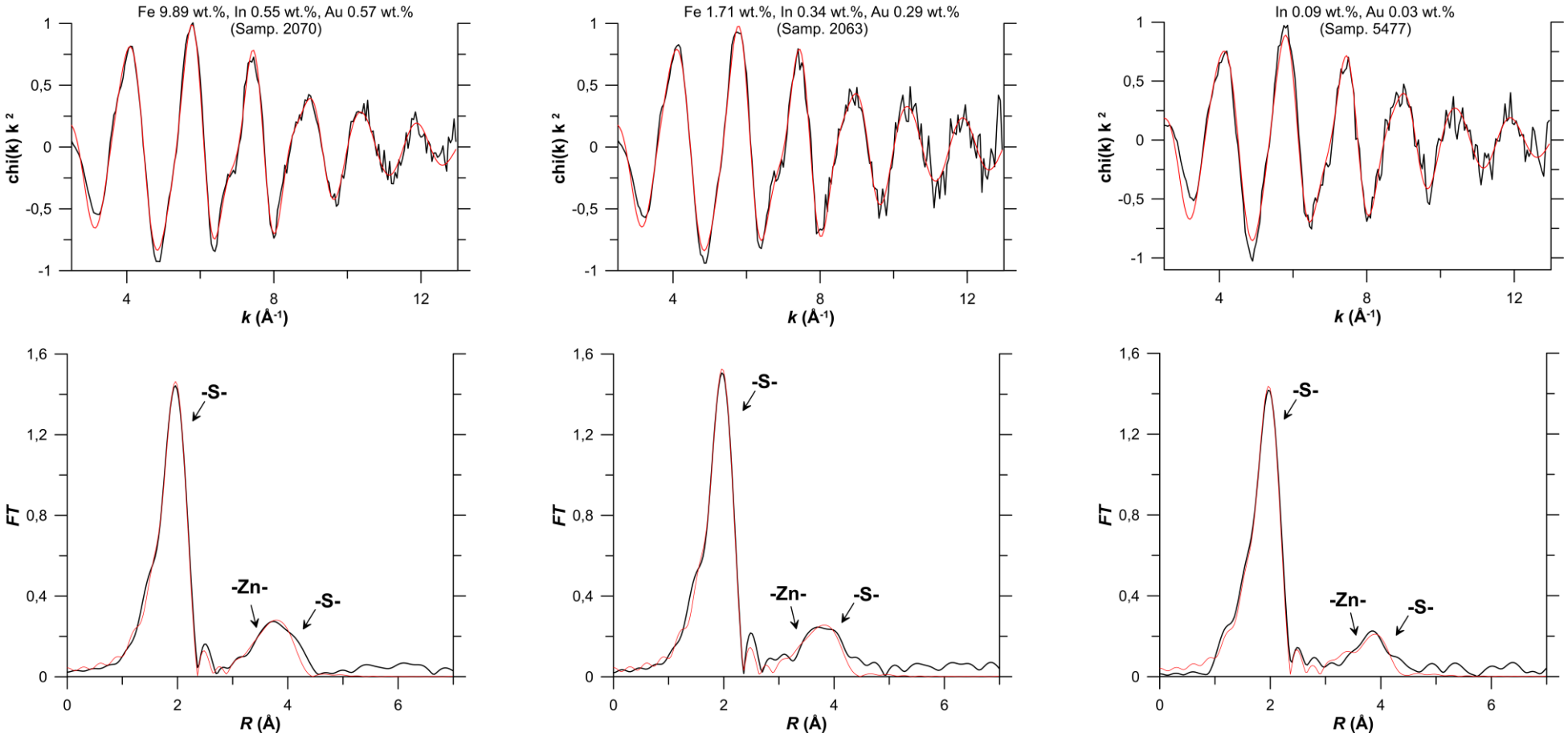
Fe 9.89 wt.%, In 0.55 wt.%, Au 0.57 wt.%
(Samp. 2070)
Fe 1.71 wt.%, In 0.34 wt.%, Au 0.29 wt.%
(Samp. 2063)
In 0.09 wt.%, Au 0.03 wt.%
(Samp. 5477)
chi(k) k ²
k (Å⁻¹)
FT
R (Å)
-S-
-Zn-
-S-

Fig. 4a.

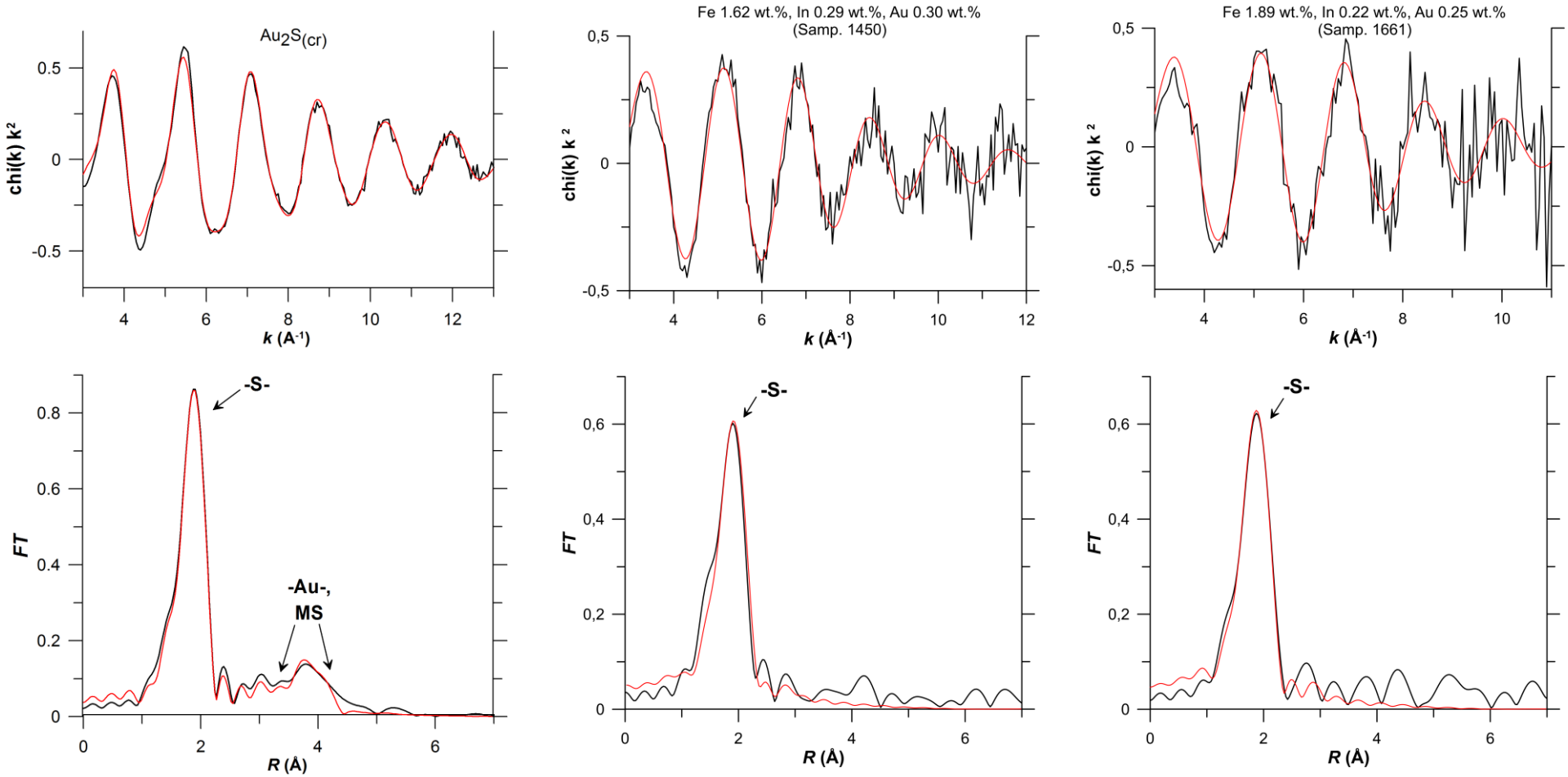
Au2S(cr)
Fe 1.62 wt.%, In 0.29 wt.%, Au 0.30 wt.%
(Samp. 1450)
Fe 1.89 wt.%, In 0.22 wt.%, Au 0.25 wt.%
(Samp. 1661)
chi(k) k²
chi(k) k ²
k (Å-1)
FT
R (Å)
-S-
-Au-,
MS

Fig. 4b.

a

Samp. 1450

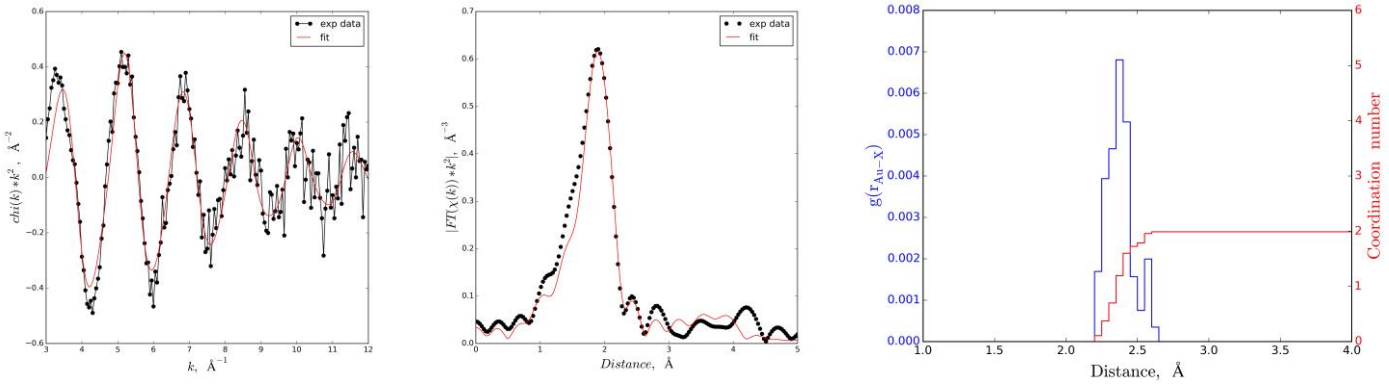

b

Samp. 1661

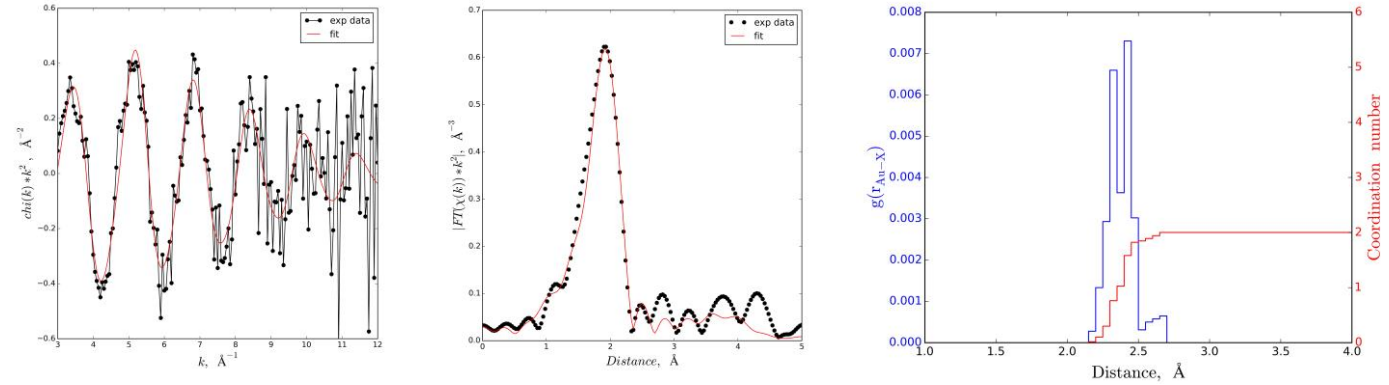

Fig. 5.

Table

Table 1. Compositions of synthetic sphalerites used in XAS experiments. Concentrations are given in wt% (± 2σ).

Sample No	EPMA[3]										LA-ICP-MS
	Zn	In	Fe	S	Au	Cd	Mn	Se	Total	Empirical formula	Au
2070[1]	54.97 (1.59)	0.55 (0.01)	9.89 (0.03)	33.16 (0.28)	0.57 (0.01)	n/d	n/d	n/d	99.14 (1.74)	$(Zn_{0.94},Fe_{0.05})S_{1.01}$	0.560 (0.015)
2063[1]	63.89 (1.00)	0.34 (0.02)	1.71 (0.07)	33.06 (0.57)	0.29 (0.03)	n/d	n/d	n/d	99.29 (1.69)	$(Zn_{0.96},Fe_{0.03})S_{1.01}$	0.310 (0.004)
5477[1]	65.84 (1.26)	0.09 (0.02)	n/d	33.69 (0.69)	0.03 (0.02)	n/d	n/d	n/d	99.65 (1.99)	$Zn_{0.98}S_{1.02}$	0.035 (0.003)
1440[2]	64.74 (1.06)	n/d	1.49 (0.02)	33.81 (0.59)	n/d	n/d	n/d	n/d	100.04 (1.30)	$(Zn_{0.95},Fe_{0.03})S$	0.020 (0.003)
1450[2]	63.95 (0.51)	0.29 (0.02)	1.62 (0.13)	33.73 (0.32)	0.30 (0.05)	0.48 (0.11)	0.24 (0.05)	0.13 (0.07)	100.74 (0.59)	$(Zn_{0.95},Fe_{0.03})S$	0.29 (0.05)
1661[1]	65.24 (0.31)	0.22 (0.03)	1.89 (0.06)	33.76 (0.53)	0.25 (0.05)	n/d	n/d	n/d	101.36 (0.55)	$(Zn_{0.96},Fe_{0.03})S_{1.01}$	0.21 (0.05)

[1] Salt flux synthesis method; [2] gas transport synthesis method; [3] n/d = not determined.

Table 2. Positions of edge jump (e.j.) and the first intense feature (white line, WL) of In *K*-edge and Au L_3-edge spectra recorded for of Au±In-bearing sphalerites and standards (±0.5 eV).

Sample, standard	Feature	Position, eV
In K-edge XANES		
In_2O_3	e.j. WL	27942.7 27949.1
In_2S_3	e.j. WL	27940.9 27946.9
Sample 2063 Fe 1.71 wt%, In 0.34 wt%, Au 0.31 wt%	e.j. WL	27942.0 27948.1
Sample 2070 Fe 9.89 wt%, In 0.55 wt%, Au 0.56 wt%	e.j. WL	27942.0 27948.1
Sample 5477 In 0.09 wt%, Au 0.035 wt%	e.j. WL	27941.5 27948.2
Au L_3-edge HERFD-XANES		
Au	e.j.	11919.3 11922.0
Au_2S	e.j.	11919.3 11921.3
Sample1440 Fe 1.49 wt%, Au 0.02 wt%	e.j.	11919.8 11922.5
Sample1450 Fe 1.62 wt%, In 0.29 wt%, Au 0.29 wt%	e.j. WL	11919.8 11922.3
Sample1661 Fe 1.89 wt%, In 0.22 wt%, Au 0.21 wt%	e.j. WL	11920.3 11922.8

Table 3. Indium, gold, and iron local atomic structure in sphalerite determined by EXAFS fitting using IFEFFIT package (fit in *k*-space unless otherwise indicated, k^2 weighting). Numbers without uncertainties were fixed during the fit. Uncertainties are calculated by ARTEMIS program.

Scattering atoms	*N*	*r*, Å	σ^2, Å^{-2}	E^0, eV	R-factor
Zn K-edge[1]					
Synthetic sphalerite (gas transport synthesis), *k*-space: 2.5 – 13					
S	4	2.34±0.01	0.005±0.001		
Zn	12	3.84±0.01	0.015±0.001	4.0±0.6	0.012
S	12	4.46±0.02	0.018±0.003		
Sample 2070 (Fe 9.89 wt.%, In 0.55 wt.%, Au 0.57 wt%), *k*-space: 2.5 – 13					
S	4.00±0.44	2.34±0.01	0.005±0.001		
Zn	12	3.84±0.02	0.015±0.002	4.5±1.0	0.045
S	12	4.45±0.03	0.018±0.005		
Sample 2063 (Fe 1.71 wt.%, In 0.34 wt.%, Au 0.29 wt%), *k*-space: 2.5 – 13					
S	3.84±0.44	2.34±0.01	0.005±0.001		
Zn	12	3.84±0.02	0.015±0.002	5.0±1.1	0.048
S	12	4.45±0.03	0.017±0.005		
Sample 1450 (Fe 1.62 wt.%, In 0.29 wt.%, Au 0.30 wt%), , *k*-space: 2.5 – 13					
S	3.82±0.45	2.34±0.01	0.005±0.001		
Zn	12	3.84±0.02	0.015±0.002	5.1±1.1	0.051
S	12	4.45±0.03	0.017±0.005		
Sample 1661 (Fe 1.89 wt.%, In 0.22 wt.%, Au 0.25 wt%), *k*-space: 2.5 – 13					
S	4.04±0.45	2.34±0.01	0.005±0.001		
Zn	12	3.84±0.02	0.015±0.002	5.0±1.0	0.047
S	12	4.45±0.03	0.016±0.005		
Fe K-edge[2]					
Sample 2070, *k*-space: 2.5 – 11					
S	3.68±0.54	2.34±0.01	0.003±0.002		
Zn	12	3.84±0.02	0.016±0.003	2.7±1.3	0.051
S	12	4.42±0.04	0.017±0.007		
Sample 2063, *k*-space: 2.5 – 11					
S	4.26±0.82	2.34±0.01	0.003±0.002		
Zn	12	3.83±0.03	0.014±0.004	1.3±1.8	0.081
S	12	4.40±0.05	0.015±0.008		
Sample 1450, *k*-space: 2.5 – 10					
S	4.84±1.45	2.34±0.02	0.003±0.003		
Zn	12	3.81±0.04	0.012±0.004	2.6±3.3	0.097
S	12	4.40±0.15	0.027±0.032		
Sample 1661, *k*-space: 2.5 – 11					
S	3.75±0.81	2.34±0.01	0.001±0.002		
Zn	12	3.83±0.03	0.013±0.003	2.5±2.1	0.087
S	12	4.43±0.08	0.022±0.015		
In K-edge[3]					
Sample 2063, *k*-space: 2.5 – 13					
S	4.22±0.46	2.46±0.01	0.004±0.001		
Zn	12	3.92±0.03	0.018±0.004	5.5±1.2	0.049
S	12	4.48±0.04	0.016±0.006		
Sample 2070, *k*-space: 2.5 – 13					
S	4.46±0.35	2.46±0.01	0.005±0.001		
Zn	12	3.92±0.02	0.018±0.002	5.0±0.9	0.026
S	12	4.48±0.03	0.015±0.004		
Sample 5477 (In 0.09 wt.%, Au 0.03 wt%), *k*-space: 2.5 – 13					
S	4.23±0.52	2.46±0.01	0.005±0.001		
Zn	12	3.93±0.04	0.020±0.005	6.2±1.3	0.057
S	12	4.46±0.05	0.017±0.008		

Table 3. – continued.

Au L_3-edge[4]					
Au_2S, synthetic, *k*-space: 3– 13					
S Au	2 6	2.30±0.005 3.75±0.08	0.0040±0.0003 0.03±0.02	5.1±0.7	0.017
Sample 1450, *k*-space: 3 – 12, fitting in R-space: 1.2-3.0.					
S	2.39±0.27	2.35±0.01	0.008±0.001	0.4±1.3	0.015
Sample 1661, *k*-space: 3 – 11, fitting in R-space: 1.2-3.0					
S	2.48±0.34	2.35±0.01	0.008±0.002	0.7±1.5	0.018

[1] $S_0^2 = 0.85$
[2] $S_0^2 = 0.75$
[3] Sphalerite structure from Jamieson and Demarest (1980) was used as initial model for EXAFS fitting, $S_0^2 = 0.95$ was calculated from fitting of In_2S_3 model spectra;
[4] Au_2S structure (Ishikawa et al., 1995) was used as initial model for EXAFS fitting, the value of $S_0^2 = 0.84$ calculated from fitting of Au_2S model spectra was used for fitting of Au-In-sphalerite spectra.